Reemergent Superconductivity and Avoided Quantum Criticality in Cd-Doped $CeIrIn_5$ under Pressure

Y. Chen,[1] W. B. Jiang,[1] C. Y. Guo,[1] F. Ronning,[2] E. D. Bauer,[2] Tuson Park,[3] H. Q. Yuan,[1,4] Z. Fisk,[5] J. D. Thompson,[2] and Xin Lu[1,4,*]

[1]*Center for Correlated Matter and Department of Physics, Zhejiang University, Hangzhou 310058, China*
[2]*Los Alamos National Laboratory, Los Alamos, New Mexico 87545, USA*
[3]*Department of Physics, Sungkyunkwan University, Suwon 440-746, South Korea*
[4]*Collaborative Innovation Center of Advanced Microstructures, Nanjing University, Nanjing, 210093, China*
[5]*Department of Physics, University of California, Irvine, California 92697, USA*

(Received 23 December 2014; published 9 April 2015)

We investigated the electrical resistivity and heat capacity of 1% Cd-doped $CeIrIn_5$ under hydrostatic pressure up to 2.7 GPa, near where long-range antiferromagnetic order is suppressed and bulk superconductivity suddenly reemerges. The pressure-induced T_c is close to that of pristine $CeIrIn_5$ at 2.7 GPa, and no signatures of a quantum critical point under pressure support a local origin of the antiferromagnetic moments in Cd-$CeIrIn_5$ at ambient pressure. Similarities between superconductors $CeIrIn_5$ and $CeCoIn_5$ in response to Cd substitutions suggest a common magnetic mechanism.

DOI: 10.1103/PhysRevLett.114.146403 PACS numbers: 71.27.+a, 74.25.Dw, 74.40.Kb, 74.62.-c

For over a decade, the $CeMIn_5$ (M = Co, Rh, Ir) heavy fermion materials have served as prototypes for exploring the relationship between magnetism and unconventional superconductivity [1,2]. As an example, superconductivity that develops at atmospheric pressure below $T_c \sim 2.3$ K in $CeCoIn_5$ [3] emerges from a non-Fermi-liquid normal state with properties consistent with those expected at an antiferromagnetic (AFM) quantum critical point (QCP) [4,5]. A minor amount of Cd substitution into In sites of $CeCoIn_5$ destroys superconductivity (SC) and induces long-range AFM order, while applying physical pressure tunes the system back to a bulk superconducting state [6]. Cd-doping and pressure are thus naively interpreted as complementary tuning parameters for $CeCoIn_5$. Nuclear magnetic resonance (NMR) experiments on Cd-doped $CeCoIn_5$, however, challenge this simple interpretation [7]: droplets of magnetic order, with a magnetic correlation length of a few lattice constants, nucleate around Cd impurities. Above a critical concentration of Cd at which the Cd-Cd separation equals a magnetic correlation length, long-range magnetic order develops but is suppressed by pressure, due to a systematic reduction of the magnetic correlation length [8], and leaves a heterogeneous electronic state [9] without the signatures of quantum criticality present in pristine $CeCoIn_5$. This unusual response of $CeCoIn_5$ to Cd-doping and pressure is a consequence of antiferromagnetic quantum fluctuations freezing around Cd impurities and provides further evidence that superconductivity is mediated by magnetic fluctuations [10,11]. Cd is not unique in inducing long-range magnetic order in $CeCoIn_5$. Hg-doping produces almost identical results [12]. In contrast, Sn-doping does not induce magnetic order; it monotonically suppresses superconductivity in $CeCoIn_5$ and Fermi liquid properties emerge. These contrasting effects of Cd/Hg and Sn substitutions are due to differences in local hybridization. As shown by density functional theory [13] and dynamical mean field [8] calculations, the average hybridization between Ce f and conduction electrons is locally weaker around Cd but stronger around Sn dopants, the former favoring and the latter adverse to the formation of magnetic droplets.

Though experiments clearly point to magnetically mediated superconductivity in $CeCoIn_5$ and in $CeRhIn_5$ under pressure [14,15], the mechanism of superconductivity in $CeIrIn_5$, the other member of the $CeMIn_5$ family with $T_c \sim 0.4$ K [16], has remained controversial. NMR [17] as well as thermodynamic and transport measurements [18] are consistent with $CeIrIn_5$ being in close proximity to an AFM QCP, which suggests a magnetic pairing mechanism. In contrast, nuclear quadrupole (NQR) experiments have been interpreted as providing evidence for pairing mediated by valence fluctuations [19]. Similar to the case of $CeCoIn_5$, Cd doping in $CeIrIn_5$ induces long-range AFM order with $T_N \sim 2.3$ K for 0.75% actual Cd concentration [6]. Interestingly, for a given Cd concentration, T_N is notably higher in $CeIrIn_5$ than in $CeCoIn_5$ [6], suggesting that $CeIrIn_5$ prefers to be magnetic even more so than $CeCoIn_5$. Whereas, this also favors the possibility of magnetic pairing, NQR studies of the pressure-induced superconductivity in Cd-doped $CeIrIn_5$ find an unexpectedly large residual spin-lattice relaxation rate T_1^{-1} that is linear in temperature well below T_c, which also could be consistent with valence fluctuations playing a prominent role in producing superconductivity [19]. With this controversy, other experimental techniques are required to explore the pairing mechanism in $CeIrIn_5$.

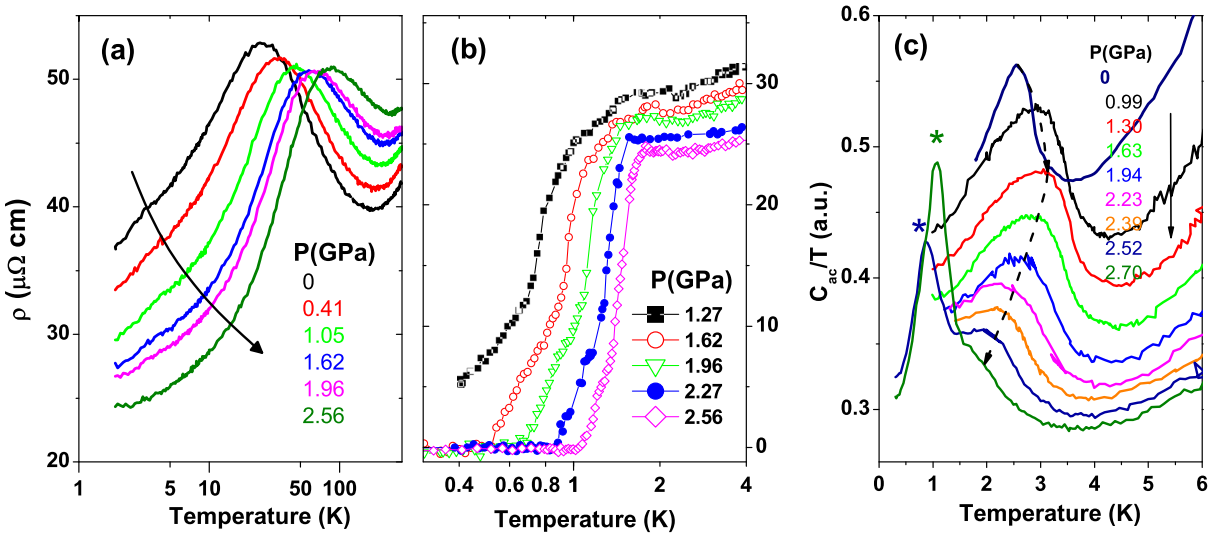

FIG. 1 (color online). Pressure evolution of (a) electrical resistivity between 1.8 and 300 K; (b) electrical resistivity between 0.4 and 4 K; (c) heat capacity of 1% Cd doped $CeIrIn_5$. The heat capacity curves measured by ac calorimetry are in arbitrary units and shifted vertically for clarity, while the low temperature data ($T < 1$ K) for $P \leq 2.39$ GPa have no additional transitions and are not shown to avoid confusion. The dashed line in (c) is a guide to eyes to track the AFM T_N evolution under pressures and the superconducting transitions are marked by $\star$ for 2.53 and 2.70 GPa.

In this Letter, we report electrical resistivity and heat capacity measurements on $CeIr(In_{1-x}Cd_x)_5$ as a function of pressure and construct its corresponding temperature-pressure phase diagram, where bulk superconductivity emerges abruptly around 2.5 GPa and signatures of quantum criticality are absent in the vicinity of the pressure where T_N extrapolates to $T = 0$. These observations, together with existing NQR experiments and recent determinations of the orbital anisotropy of the $4f$ wave function in $CeIrIn_5$ [20], provide a new, consistent interpretation of the physics of $CeIrIn_5$ and the mechanism of unconventional superconductivity in it.

Single crystals of $CeIr(In_{1-x}Cd_x)_5$ ($x = 1.0\%$ is the actual Cd concentration) were grown by the self-flux method as described elsewhere [6] and screened to ensure the absence of free In. We checked the specific heat of different crystals from the same batch and the measured T_N scattered in a small range between 2.6 and 2.9 K as shown in Fig. 1 of the Supplemental Material [21], consistent with the reported long-range AFM Néel temperature $T_N \sim 2.8$ K for this Cd concentration [6]. Because T_N is extremely sensitive to the Cd doping level, these measurements confirm a reasonably uniform distribution of Cd dopants inside $CeIrIn_5$ during crystal growth. For pressure measurements, the screened crystals were mounted in a piston-cylinder-type pressure cell with silicone fluid as the pressure transmitting medium to achieve a nearly hydrostatic pressure up to 2.7 GPa. The pressure at low temperature was determined from the resistive superconducting transition of Pb. The electrical resistivity was measured by a conventional four-probe method and the heat capacity C_{ac} of $CeIr(In_{1-x}Cd_x)_5$ under pressure was derived from an ac calorimetric technique, where a heater glued on the sample generates a small temperature oscillation ΔT by flowing an ac current and a chromel-AuFe (0.07%) thermocouple glued on the opposite side senses an ac voltage signal proportional to ΔT [24].

Figure 1 shows the pressure evolution of temperature-dependent electrical resistivity [high—panel (a) and low—panel (b) temperatures] and in panel (c) the heat capacity for 1.0% Cd-doped $CeIrIn_5$. The room-temperature resistivity increases monotonically with pressure and the coherence peak, typical in heavy Fermion materials, also shifts to higher temperatures, signaling enhanced hybridization between Ce f electrons and conduction electrons. As shown in Fig. 1(c), the T_N determined by ac calorimetry reaches its maximum value 3.1 K near 1.3 GPa and then gradually decreases; however, it still survives with a noticeable hump at 2.7 GPa, the highest pressure available. Interestingly, superconductivity suddenly emerges at 2.5 GPa with a bulk $T_c \sim 0.8$ K and T_c reaches 1.0 K at 2.7 GPa, which is very similar to pure $CeIrIn_5$ [25] even though the Cd-doped material has a much larger residual resistivity ρ_0. However, a SC resistive transition appears already at 1.27 GPa in Fig. 1(b), much lower than the pressure for bulk SC to appear, even though the resistive transition itself is broad and does not reach zero above 0.4 K. At 2.56 GPa, the temperature at which the resistive SC transition reaches zero resistance is very close to the bulk T_c in heat capacity. The obvious T_c distinctions at low pressures imply an initial emergence of filamentary superconductivity and its final development into bulk SC, which is commonly observed in other heavy fermion systems due to the coexisting magnetism [26,27]. A much higher resistive

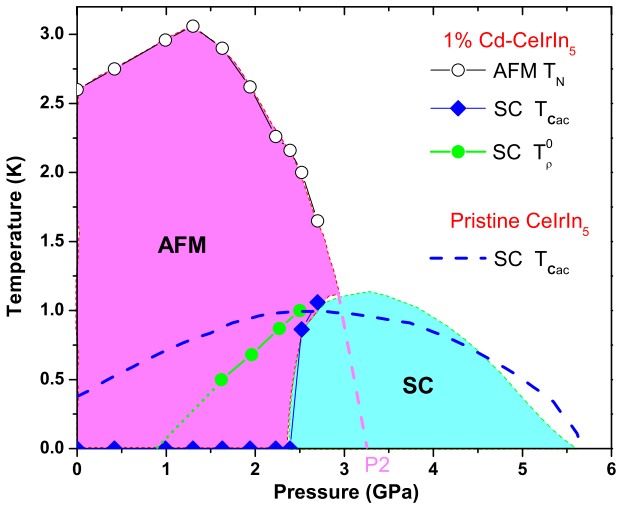

FIG. 2 (color online). Temperature-pressure (T-P) phase diagram of 1% Cd-$CeIrIn_5$. The AFM T_N is determined by ac calorimetry while superconducting transition temperatures T_c determined by resistivity and heat capacity show distinctive pressure behaviors. SC regions above 2.7 GPa are assumed as guide to eyes and a T_c curve for pristine $CeIrIn_5$ under pressure [28] is included for comparison.

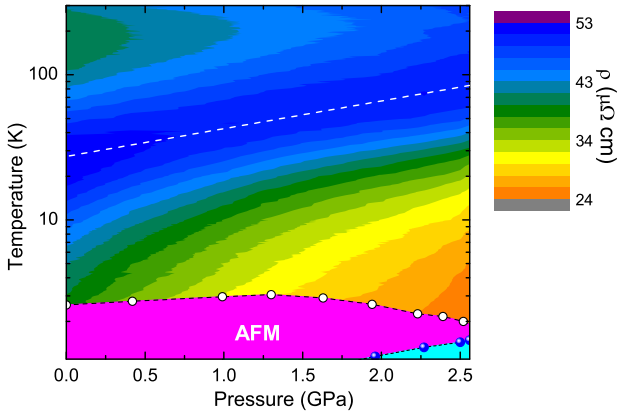

FIG. 3 (color online). The temperature-pressure contour color plot of resistivity for 1.0% Cd-doped $CeIrIn_5$ with both AFM and resistive SC boundaries included. The dashed line is a guide to eyes to track the pressure evolution of the Kondo lattice coherence temperature.

transition also is found in pure $CeIrIn_5$ at atmospheric pressure [16], but it coincides with the bulk SC transition at high pressures [25,28]. We return to this point later.

The temperature-pressure (T-P) phase diagram of 1.0% Cd-doped $CeIrIn_5$ is summarized in Fig. 2 and is in good agreement with the one proposed from NQR measurments [19]. The emergent SC phase is in the vicinity of the projected pressure $P2$, where AFM is extrapolated to vanish. This T-P phase diagram is remarkably similar to the case of $CeRhIn_5$ [14,29], leading to a speculation that SC in Cd-$CeIrIn_5$ is also induced by spin fluctuations in proximity to an AFM QCP. If so, Cd-doping and pressure are globally complementary tuning parameters: pressure reverses the effect of Cd substitution. However, Cd-$CeIrIn_5$ under pressure does not revert to pure $CeIrIn_5$ at ambient pressure ($T_c \sim 0.4$ K), but instead once magnetic order is suppressed at 2.7 GPa, the T_c of Cd-$CeIrIn_5$ is almost identical to that of pristine $CeIrIn_5$ under this pressure. Additionally, the magnitude and temperature dependence of the spin-lattice-relaxation rate $1/T_1$ also coincide in the paramagnetic states for both 0.75% Cd-doped and pure $CeIrIn_5$ at 2.7 GPa [19], suggesting a minor influence of Cd dopants on the spin fluctuation spectrum. These observations can be understood straightforwardly in the framework of the same magnetic-droplet model that successfully accounts for the role of Cd dopants in $CeCoIn_5$ [8], in particular, that antiferromagnetic quantum fluctuations are removed around Cd impurities leaving an electronically heterogeneous state but sufficient spectral weight remains in the magnetic fluctuation spectrum to produce a T_c that is nearly the same as in undoped $CeIrIn_5$.

In order to further confirm that the emergent SC in Cd-$CeIrIn_5$ is not associated with a QCP either of a magnetic or of a valence instability type, a contour color map of the resistivity magnitude as a function of temperature and pressure is plotted in Fig. 3. The resistive coherence temperature increases linearly with pressure, but the resistivity above a phase transition decreases monotonically upon approaching $P2$, resembling Cd-doped $CeCoIn_5$ under pressure [8]. This is in sharp contrast to the resistive behaviors observed in both $CeRhIn_5$ [15] and $CePt_2In_7$ [27], where the low-temperature resistivity peaks around T_c^{Max}, $P2$. In particular, the absence of a maximum low-temperature resistivity near P_2 is at odds with a valence-instability scenario for which theory predicts a large increase in residual resistivity due to scattering by critical valence fluctuations [30]. Though our highest pressure does not quite reach $P2$, the absence of a pressure-induced QCP in Cd-doped $CeIrIn_5$ is strongly suggested by the results illustrated in Fig. 3 and its similarity with the resistive behavior of pristine $CeIrIn_5$ under pressure (Refer to Figs. 2 and 3 in the Supplemental Material for more information).

Having ruled out either an AFM QCP or the presence of critical valence fluctuations near $P2$ in Cd-$CeIrIn_5$, we return to the broader questions of the physics of $CeIrIn_5$, its mechanism of superconductivity, and why its maximum T_c is only half that of other family members. We begin by comparing the behaviors of Cd-doped with Rh-doped $CeIrIn_5$, where isoelectric Rh doping also induces an AFM ground state in $CeIr_{1-x}Rh_xIn_5$ for $x \geq 0.6$ and a dome of SC appears inside the AFM phase as shown in Fig. 4 [31]. Interestingly, $CeIr_{1-x}Rh_xIn_5$ shows a cusplike minimum in its T_c at $x = 0.1$ with two separate SC domes nearby [32], leading to speculation that the SC pairing in $CeIrIn_5$ is not due to spin fluctuations but instead due to valence fluctuations [19,33]. As discussed already, NMR [17], as

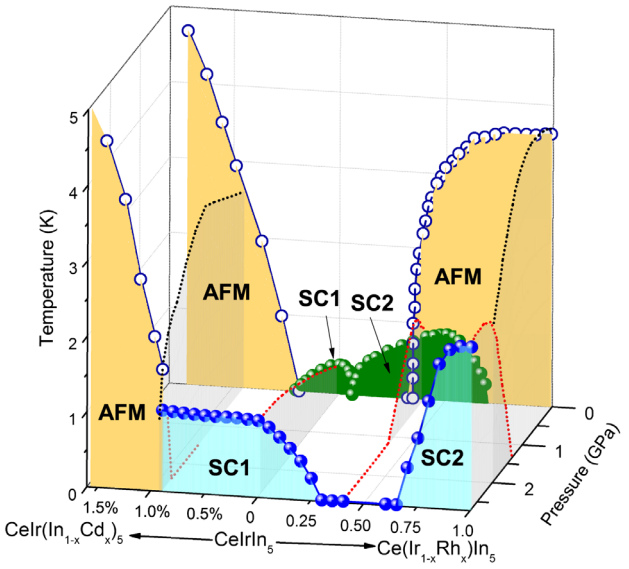

FIG. 4 (color online). 3D plot of the temperature-doping-pressure phase diagram of $CeIrIn_5$, where AFM (empty circles) and SC (solid circles) phases compete or coexist. The dotted lines are guides to eyes to track the pressure evolution of AFM or SC in different samples, i.e., 1.0% Cd-doped, pure, 40% Rh-doped $CeIrIn_5$, and pure $CeRhIn_5$. The doping phase diagram at 2.7 GPa is constructed based on smooth extrapolations of our results and those in [15,19,25,32].

well as thermodynamic and transport measurements [18], and now the similarity in the pressure responses of Cd-doped $CeCoIn_5$ and $CeIrIn_5$ provide a compelling body of evidence for magnetic pairing in $CeIrIn_5$. We take this point of view, but now must ask how should the phase diagram in Fig. 4 be understood. There are two pertinent observations that provide clues. The first is the report that the evolution of magnetism and superconductivity in $CeIr_{1-x}Rh_xIn_5$ correlates with orbital anisotropy in the $4f$ wave functions [34] that is reflected in the square of the $\pm 5/2$ contribution (α^2) to the J_z component of the Γ_7 Kramer's doublet ground state. This metric decreases nonlinearly with decreasing x and saturates to a constant for $x \leq 0.3$ instead of continuing to decrease to the still smaller value for $CeCoIn_5$. Though this trend in α^2 is consistent with stronger $f-c$ hybridization in $CeIrIn_5$ than in $CeRhIn_5$ [34], it does not explain why α^2 saturates in Ir-rich compounds. As also shown in Fig. 4, the maximum T_c in $CeIr_{1-x}Rh_xIn_5$ at atmospheric pressure is 1 K, but at 2.7 GPa T_c exceeds 2 K for Rh-rich materials and does not exceed 1 K for Ir-rich or Cd-doped $CeIrIn_5$. This could be consistent with different pairing mechanisms in these extremes; however, as mentioned, a magnetic pairing mechanism appears to be operative through the phase diagram. Though a small α^2 correlates with the appearance of superconductivity, a notable difference between $CeCoIn_5$ and $CeIrIn_5$ is that Ir has a much larger atomic number ($Z = 77$) than Co ($Z = 27$) or for that matter Rh ($Z = 45$). This provides a second clue. Because spin-orbit coupling (SOC) increases as Z^4/n^3, where n is the principal quantum number, the atomically derived SOC due to Ir should be roughly 14 (4) times stronger than that in Co (Rh). The stronger alignment of spin and orbit in $CeIrIn_5$ weakens pairing of a d-wave state preferred by antiferromagnetic fluctuations [35], consistent with a lower maximum T_c in Ir-rich $CeIr_{1-x}Rh_xIn_5$ and Cd-doped $CeIrIn_5$ than in the other $CeMIn_5$ materials. The competition between superconductivity with d-wave symmetry in $CeRhIn_5$ under pressure [36,37] and a magnetically mediated superconducting state with increasingly strong SOC as the Ir concentration increases in $CeIr_{1-x}Rh_xIn_5$ provides a plausible explanation for the evolution of superconductivity shown in Fig. 4, in particular, the origin of the cusp in T_c near $x = 0.1$ at atmospheric pressure that becomes a line of compositions with no superconductivity at 2.7 GPa. Besides influencing the phase diagram, SOC also should produce additional fine structure in the electronic band structure which would allow formation of a small superconducting gap that would be destroyed easily by scattering from defects, e.g., Cd and Ir. Excitations at the extended gap zeros give rise to an increase in the T-linear contribution to T_1^{-1} without a need to invoke a role of valence fluctuations. We further note that defects are intrinsic to undoped $CeIrIn_5$ in which there is a small (~1.0%) intergrowth of a $TlAsPd_5$ structure type [38].

In conclusion, we have constructed the T-P phase diagram of 1% Cd-doped $CeIrIn_5$ based on resistivity and heat capacity measurements under pressure up to 2.7 GPa, which suppresses long-range AFM order and induces superconductivity with bulk $T_c \sim 1.0$ K, comparable to that in pristine $CeIrIn_5$ at a comparable pressure. These experiments show that there is no signature for a quantum-critical response as T_N approaches zero and are consistent with a local origin of AFM order where magnetic-droplets nucleate around Cd dopants from the freezing of quantum-critical fluctuations hosted by the parent $CeIrIn_5$. These and other experiments indicate that magnetic fluctuations mediate Cooper pairing in $CeIrIn_5$, where spin-orbit coupling plays a nontrivial role as well as in $CeIr(In_{1-x}Cd_x)_5$ and $CeIr_{1-x}Rh_xIn_5$. Knight shift measurements in the superconducting state of these materials would be worthwhile.

We acknowledge valuable discussions with Y. F. Yang, J. X. Zhu, and G. M. Zhang. Work at Zhejiang University is supported by the National Natural Science Foundation of China (Grants No. 11374257, No. 11174245), the Fundamental Research Funds for the Central Universities and National Basic Research Program of China (Grant No. 2011CBA00103). Work at Los Alamos National Laboratory was performed under the auspices of the U.S. Department of Energy, Office of Basic Energy Sciences, Division of Materials Science and Engineering.

Work at SKKU is supported by an NRF grant funded by the Korean Ministry of Education, Science and Technology (MEST) (Grants No. 2012R1A3A2048816 and No. 220-2011-1-C00014).

*Corresponding author.
xinluphy@zju.edu.cn

[1] J. L. Sarrao and J. D. Thompson, J. Phys. Soc. Jpn. **76**, 051013 (2007).
[2] J. D. Thompson and Z. Fisk, J. Phys. Soc. Jpn. **81**, 011002 (2012).
[3] C. Petrovic, P. G. Pagliuso, M. F. Hundley, R. Movshovich, J. L. Sarrao, J. D. Thompson, Z. Fisk, and P. Monthoux, J. Phys. Condens. Matter **13**, L337 (2001).
[4] V. A. Sidorov, M. Nicklas, P. G. Pagliuso, J. L. Sarrao, Y. Bang, A. V. Balatsky, and J. D. Thompson, Phys. Rev. Lett. **89**, 157004 (2002).
[5] J. Paglione, M. A. Tanatar, D. G. Hawthorn, E. Boaknin, R. W. Hill, F. Ronning, M. Sutherland, L. Taillefer, C. Petrovic, and P. C. Canfield, Phys. Rev. Lett. **91**, 246405 (2003).
[6] L. D. Pham, T. Park, S. Maquilon, J. D. Thompson, and Z. Fisk, Phys. Rev. Lett. **97**, 056404 (2006).
[7] R. R. Urbano, B.-L. Young, N. J. Curro, J. D. Thompson, L. D. Pham, and Z. Fisk, Phys. Rev. Lett. **99**, 146402 (2007).
[8] S. Seo, X. Lu, J.-X. Zhu, R. R. Urbano, N. Curro, E. D. Bauer, V. A. Sidorov, L. D. Pham, T. Park, Z. Fisk *et al.*, Nat. Phys. **10**, 120 (2014).
[9] A. J. Millis, D. K. Morr, and J. Schmalian, Phys. Rev. Lett. **87**, 167202 (2001).
[10] C. Stock, C. Broholm, J. Hudis, H. J. Kang, and C. Petrovic, Phys. Rev. Lett. **100**, 087001 (2008).
[11] J. S. Van Dyke, F. Massee, M. P. Allan, J. C. S. Davis, C. Petrovic, and D. K. Morr, Proc. Natl. Acad. Sci. (U.S.A.) **111**, 11663 (2014).
[12] C. H. Booth, E. D. Bauer, A. D. Bianchi, F. Ronning, J. D. Thompson, J. L. Sarrao, J. Y. Cho, J. Y. Chan, C. Capan, and Z. Fisk, Phys. Rev. B **79**, 144519 (2009).
[13] K. Gofryk, F. Ronning, J.-X. Zhu, M. N. Ou, P. H. Tobash, S. S. Stoyko, X. Lu, A. Mar, T. Park, E. D. Bauer *et al.*, Phys. Rev. Lett. **109**, 186402 (2012).
[14] H. Hegger, C. Petrovic, E. G. Moshopoulou, M. F. Hundley, J. L. Sarrao, Z. Fisk, and J. D. Thompson, Phys. Rev. Lett. **84**, 4986 (2000).
[15] T. Park, V. A. Sidorov, F. Ronning, J.-X. Zhu, Y. Tokiwa, H. Lee, E. D. Bauer, R. Movshovich, J. L. Sarrao, and J. D. Thompson, Nature (London) **456**, 366 (2008).
[16] C. Petrovic, R. Movshovich, M. Jaime, P. G. Pagliuso, M. F. Hundley, J. L. Sarrao, Z. Fisk, and J. D. Thompson, Europhys. Lett. **53**, 354 (2001).
[17] S. Kambe, H. Sakai, Y. Tokunaga, and R. E. Walstedt, Phys. Rev. B **82**, 144503 (2010).
[18] T. Shang, R. E. Baumbach, K. Gofryk, F. Ronning, Z. F. Weng, J. L. Zhang, X. Lu, E. D. Bauer, J. D. Thompson, and H. Q. Yuan, Phys. Rev. B **89**, 041101 (2014).
[19] M. Yashima, N. Tagami, S. Taniguchi, T. Unemori, K. Uematsu, H. Mukuda, Y. Kitaoka, Y. Ōta, F. Honda, R. Settai *et al.*, Phys. Rev. Lett. **109**, 117001 (2012).
[20] T. Willers, Z. Hu, N. Hollmann, P. O. Körner, J. Gegner, T. Burnus, H. Fujiwara, A. Tanaka, D. Schmitz, H. H. Hsieh *et al.*, Phys. Rev. B **81**, 195114 (2010).
[21] See Supplemenal Material at http://link.aps.org/supplemental/10.1103/PhysRevLett.114.146403 for data and their discussion, which includes Refs. [22, 23].
[22] Y. Nakajima, H. Shishido, H. Nakai, T. Shibauchi, M. Hedo, Y. Uwatoko, T. Matsumoto, R. Settai, Y. Onuki, H. Kontani *et al.*, Phys. Rev. B **77**, 214504 (2008).
[23] T. Hu, Y. P. Singh, L. Shu, M. Janoschek, M. Dzero, M. B. Maple, and C. C. Almasan, Proc. Natl. Acad. Sci. U.S.A. **110**, 7160 (2013).
[24] V. A. Sidorov, J. D. Thompson, and Z. Fisk, J. Phys. Condens. Matter **22**, 406002 (2010).
[25] T. Muramatsu, T. C. Kobayashi, K. Shimizu, K. Amaya, D. Aoki, Y. Haga, and Y. Onuki, Physica (Amsterdam) **388–389C**, 539 (2003).
[26] T. Park, H. Lee, I. Martin, X. Lu, V. A. Sidorov, K. Gofryk, F. Ronning, E. D. Bauer, and J. D. Thompson, Phys. Rev. Lett. **108**, 077003 (2012).
[27] V. A. Sidorov, X. Lu, T. Park, H. Lee, P. H. Tobash, R. E. Baumbach, F. Ronning, E. D. Bauer, and J. D. Thompson, Phys. Rev. B **88**, 020503 (2013).
[28] S. Kawasaki, M. Yashima, Y. Mugino, H. Mukuda, Y. Kitaoka, H. Shishido, and Y. Ōnuki, Phys. Rev. Lett. **96**, 147001 (2006).
[29] G. Knebel, D. Aoki, D. Braithwaite, B. Salce, and J. Flouquet, Phys. Rev. B **74**, 020501 (2006).
[30] K. Miyake and H. Maebashi, J. Phys. Soc. Jpn. **71**, 1007 (2002).
[31] P. G. Pagliuso, C. Petrovic, R. Movshovich, D. Hall, M. F. Hundley, J. L. Sarrao, J. D. Thompson, and Z. Fisk, Phys. Rev. B **64**, 100503 (2001).
[32] M. Nicklas, V. A. Sidorov, H. A. Borges, P. G. Pagliuso, J. L. Sarrao, and J. D. Thompson, Phys. Rev. B **70**, 020505 (2004).
[33] S. Kawasaki, G.-Q. Zheng, H. Kan, Y. Kitaoka, H. Shishido, and Y. Ōnuki, Phys. Rev. Lett. **94**, 037007 (2005).
[34] T. Willers, F. Strigari, Z. Hu, V. Sessi, N. B. Brookes, E. D. Bauer, J. L. Sarrao, J. D. Thompson, A. Tanaka, S. Wirth *et al.*, Proc. Natl. Acad. Sci. U.S.A. **112**, 2384 (2015).
[35] P. Monthoux and G. G. Lonzarich, Phys. Rev. B **63**, 054529 (2001).
[36] Y. Kohori, H. Taira, H. Fukazawa, T. Kohara, Y. Iwamoto, T. Matsumoto, and M. B. Maple, J. Alloys Compd. **408–412**, 51 (2006).
[37] T. Park and J. D. Thompson, New J. Phys. **11**, 055062 (2009).
[38] S. Wirth, Y. Prots, M. Wedel, S. Ernst, S. Kirchner, Z. Fisk, J. D. Thompson, F. Steglich, and Y. Grin, J. Phys. Soc. Jpn. **83**, 061009 (2014).